MedChemComm

Accepted Manuscript

This article can be cited before page numbers have been issued, to do this please use: K. Y. P. Apperley, I. Roy, V. Saucier, N. Brunet-Filion, S. Piscopo, C. Pardin, É. De Francesco, C. Hao and J. W. Keillor, *Med. Chem. Commun.*, 2016, DOI: 10.1039/C6MD00565A.

This is an Accepted Manuscript, which has been through the Royal Society of Chemistry peer review process and has been accepted for publication.

Accepted Manuscripts are published online shortly after acceptance, before technical editing, formatting and proof reading. Using this free service, authors can make their results available to the community, in citable form, before we publish the edited article. We will replace this Accepted Manuscript with the edited and formatted Advance Article as soon as it is available.

You can find more information about Accepted Manuscripts in the author guidelines.

Please note that technical editing may introduce minor changes to the text and/or graphics, which may alter content. The journal's standard Terms & Conditions and the ethical guidelines, outlined in our author and reviewer resource centre, still apply. In no event shall the Royal Society of Chemistry be held responsible for any errors or omissions in this Accepted Manuscript or any consequences arising from the use of any information it contains.

ROYAL SOCIETY OF CHEMISTRY

rsc.li/medchemcomm

View Article Online
DOI: 10.1039/C6MD00565A

Development of new scaffolds as reversible tissue transglutaminase inhibitors, with improved potency or resistance to glutathione addition†

Kim Y.P. Apperley[a], Isabelle Roy[b], Vincent Saucier[a], Nicholas Brunet-Filion[a], Sara-Pier Piscopo[a], Christophe Pardin[a], Élise De Francesco[a], Catherine Hao[a], Jeffrey W. Keillor[a,*]

[a]*Department of Chemistry and Biomolecular Sciences*
University of Ottawa
10 Marie-Curie Pvt.
Ottawa, Ontario K1N 6N5
Canada
[b]*Département de chimie*
Université de Montréal
C. P. 6128, Succursale Centre-ville
Montréal, Québec H3C 3J7
Canada
*Corresponding author: jkeillor@uottawa.ca

Keywords
tissue transglutaminase; enzyme inhibition; cinnamoyl; triazole; glutathione

† The authors declare no competing interests.

View Article Online
DOI: 10.1039/C6MD00565A

Abstract

Previous studies within our group have yielded a class of cinnamoyl-based competitive reversible inhibitors for tissue transglutaminase (TG2), with K_i values as low as 1.0 μM (compound **CP4d**). However, due to the electrophilic nature of their alkene moiety, this class of inhibitors is susceptible to nucleophilic attack by glutathione, a key element in cellular metabolism and toxicity response. To address this issue, we made several modifications to the inhibitor scaffold, ultimately showing that a bis(triazole) scaffold increased resistance to nucleophilic attack, with compound **27d** being the most potent (K_i = 10 μM). In the process of reducing reactivity, we also prepared a new class of inhibitors, replacing the alkene of **CP4d** with an alkyne, leading to a significant increase in potency for compound **22b** (K_i = 420 nM).

View Article Online
DOI: 10.1039/C6MD00565A

Introduction

Transglutaminases (E.C. 2.3.2.13) are a family of calcium-dependent enzymes that natively catalyse the crosslinking of proteins, through the formation of N^{ε}(γ-glutamyl)lysine bridges between glutamine and lysine residues. In the absence of a lysine (or acyl-acceptor amine), transglutaminases can also hydrolyse glutamine side chains to form glutamate. Tissue transglutaminase (TG2), as its name implies, is ubiquitously expressed in tissues. On the cell surface and in the extracellular matrix, TG2 adopts an open[1, 2] conformation in the presence of calcium (Ca^{2+}), its coenzyme required for transamidation[3]. Extracellular TG2 may also be deactivated[4] by disulfide bond formation, even in the presence of Ca^{2+}. In the cytosol, where the concentration of free calcium is low, and the concentration of guanine nucleotides is high, TG2 is allosterically regulated[5] to adopt a closed conformation in which it functions as a G-protein[6].

Human TG2 (hTG2) plays many physiological roles, acting in cellular differentiation[7, 8], apoptosis[9, 10], and extracellular matrix assembly[11], and it can also function as an adhesion receptor[12]. However, the up-regulation of TG2-mediated acyl-transfer has been implicated in several physiological disorders[13], such as fibrosis, cancer, and celiac disease. In light of these pathological roles, our group has studied the development of inhibitors against TG2[14-16], leading to the discovery of a family of cinnamoyl derivatives that function as reversible inhibitors. Our original studies were done using guinea pig liver TG2 (gplTG2), which displays high sequence homology with the human enzyme and a much greater solubility when expressed in recombinant form, and was therefore used as a model. The most potent inhibitors of those studies were based on a nitrocinnamoyl scaffold, such as **CP30a**[15], **CP15a**[15], ***m*-CP30a**[17] and **CP4d**[16], whose IC_{50} values are indicated in Figure 1. Following the development of a protocol for the expression and purification of hTG2 within our group, we began to work with the human form of the enzyme,

View Article Online
DOI: 10.1039/C6MD00565A

and confirmed[17] that the kinetic parameters such as K_M and K_i values are comparable when determined under similar reaction conditions. Earlier inhibition results are therefore shown with gplTG2, while the later ones were obtained with hTG2.

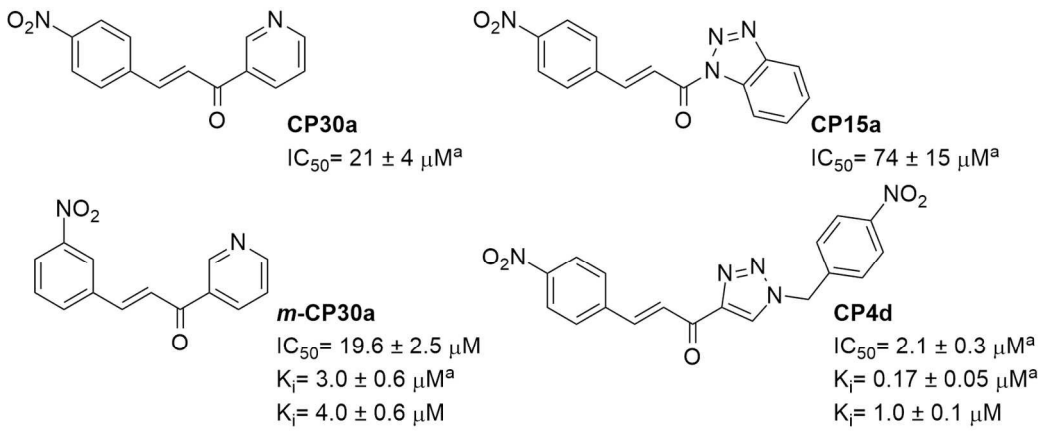

Figure 1. 4-nitrocinnamoyl-based reversible inhibitors for TG2

[a]IC_{50} value determined with gplTG2

Although these parent compounds are reversible inhibitors of TG2, they do contain an electrophilic α,β-unsaturated carbonyl motif, which may undergo Michael addition with nucleophiles such as glutathione (GSH), a tripeptide thiol whose intracellular concentration is in the millimolar range. This reaction may result in a loss of potency *in vivo*; we therefore sought to determine the extent of this reactivity, and to develop a family of inhibitors that would not be susceptible to this potential nucleophilic attack.

In this work, we started from these known scaffolds and made modifications to the electrophilic moiety to reduce its reactivity. In a first approach, we added sterically hindering groups or increased electron density at the suspected reactive site; the replacement of a carbon-carbon double bond by a triple bond resulted in a significant increase in potency, with compound **22b** being a competitive inhibitor with a K_i of 420 nM. In a second approach, we incorporated

View Article Online
DOI: 10.1039/C6MD00565A

the electrophilic alkene into a heteroaromatic group, resulting in increased resistance to nucleophilic attack by glutathione, shown for compound **27d**.

Results

GSH susceptibility of lead compounds

To test directly for reactivity with GSH, an incubation experiment was designed, using ***m*-CP30a**[18] (Figure 1) as a representative inhibitor for suspected Michael acceptors. Inhibitor ***m*-CP30a** was developed and evaluated[17] directly against hTG2, displaying an IC_{50} of 19.6 ± 2.5 μM. The reaction of ***m*-CP30a** with glutathione in DMSO, the standard conditions for measuring such reactivity[19], was followed by ^{1}H NMR by monitoring for changes from the spectra of the starting materials (see Figure S1 in SI). The mass of the formed adduct (Scheme 1) was then verified by HRMS, confirming mono-addition. After only ten minutes, the reaction between ***m*-CP30a** and GSH had proceeded to a significant extent, and after one hour, the reaction was complete, with no further changes after an additional three hours, suggesting significant GSH susceptibility within this class of inhibitors. A similar reactivity was observed with **CP4d** (see Figure S2), where the reaction was more than 50% complete after 10 minutes.

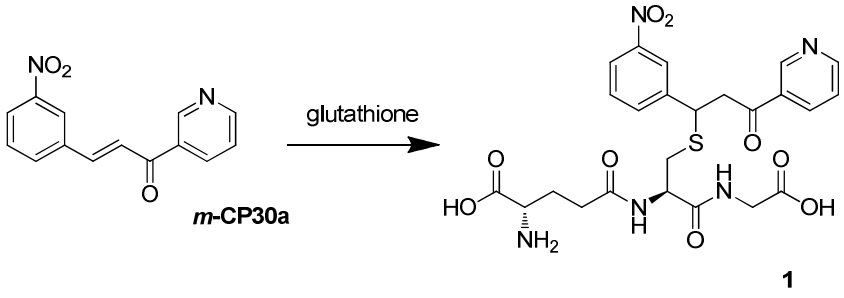

Scheme 1. Suspected adduct formation between ***m*-CP30a** and glutathione

View Article Online
DOI: 10.1039/C6MD00565A

Synthesis and evaluation of inhibitor analogues

Cβ-Alkylated analogues of **CP4d**

Several compounds were therefore designed to mimic known inhibitors, while decreasing their electrophilicity and susceptibility towards attack by GSH. Our first design featured the alkylation of the β-position of the cinnamoyl scaffold, while retaining a common benzotriazole group for comparison with parent compound **CP15a**[15] (Figure 1). Both methyl derivative **3** and isopropyl derivatives **8** & **9** (Figure 2) were synthesized by a similar approach (see Scheme S1 in SI), starting with a Horner-Wadsworth-Emmons reaction from, respectively, 4-nitrophenyl methyl and 4-nitrophenyl isopropyl ketones to afford the ethyl esters. While the diastereomers of the methyl derivative were not successfully separated, their ratio of 1:1 was determined by ^{13}C NMR spectroscopy by comparison of peak intensities. However, the isopropyl diasteromers **4** and **5** (Scheme S1) were successfully separated by flash column chromatography and identified by NOESY, based on the interaction between the vinylic proton and the neighbouring protons on one of the methyl groups. These esters were then saponified to yield the corresponding carboxylic acids (**2**, **6**, and **7**; Scheme S1), according to a literature protocol[20]. Reaction with oxalyl chloride led to the corresponding acyl chlorides, which were coupled directly with benzotriazole to afford products **3**, **8** and **9**.

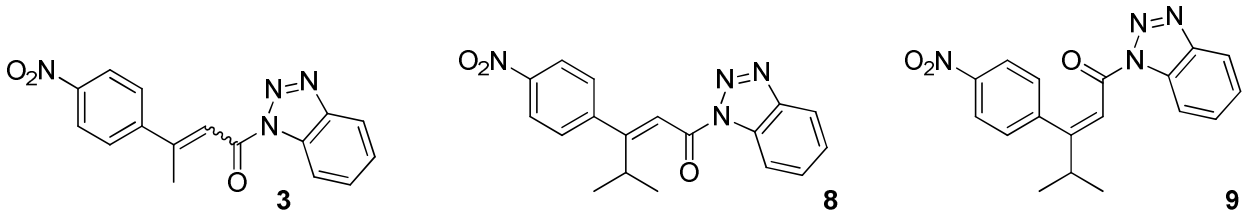

Figure 2. Cβ-Alkylated analogues of **CP4d**

View Article Online
DOI: 10.1039/C6MD00565A

Coumarin analogue of **CP15a**

Coumarin derivative **11** (Scheme 2) was designed as an alternative analogue in which the α,β-unsaturation was incorporated into an aromatic cycle. Precursor **10** was prepared[18] according to a published procedure[21] and reacted directly with thionyl chloride to form the corresponding acyl chloride, which was coupled with benzotriazole to form **11**.

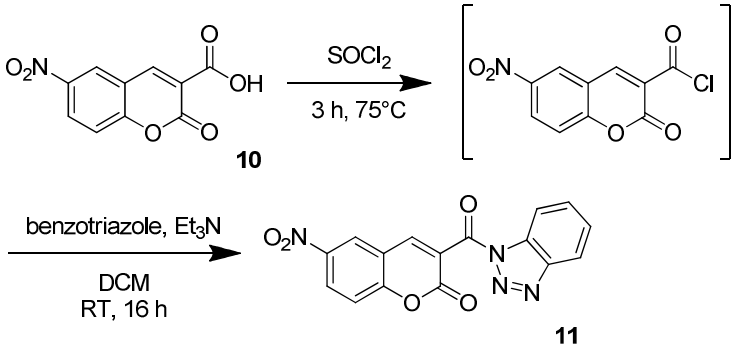

Scheme 2. Synthesis of coumarin derivative **11**

Alkyne analogue of **CP15a**

In a different approach, the cinnamoyl double bond was replaced with a triple bond (Scheme 3). Sonogashira coupling[22, 23] between 1-iodo-4-nitrobenzene and ethyl propynoate led to ester **12**, which was saponified to the corresponding carboxylic acid **13**. The acid chloride was then formed[24] *in situ* prior to coupling with benzotriazole to obtain compound **14**, an alkyne analogue of **CP15a**. The inhibition results for these benzotriazole compounds are gathered in Table 1.

View Article Online
DOI: 10.1039/C6MD00565A

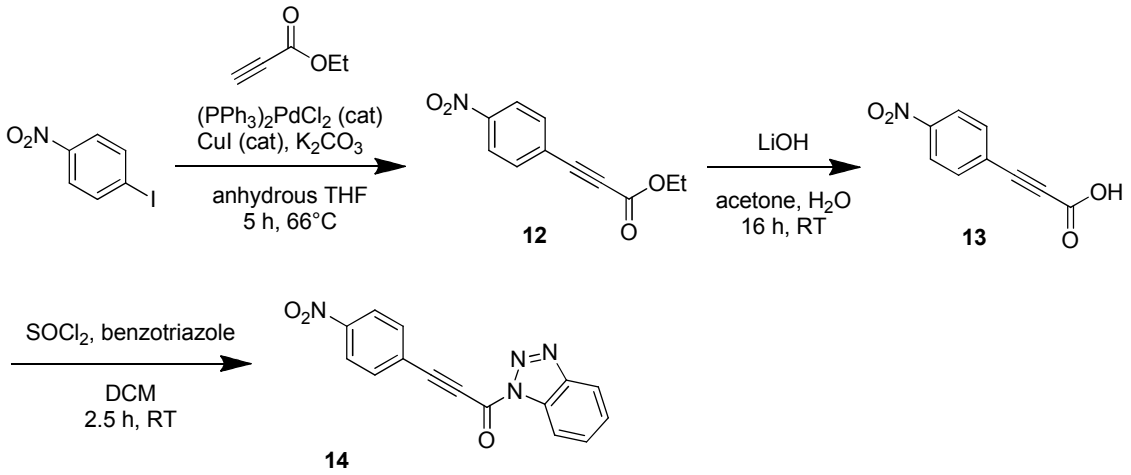

Scheme 3. Synthesis of alkynyl derivative **14**

Table 1. IC_{50} values for analogues of benzotriazole **CP15a**

Compound	IC_{50} (μM)
CP15a	74 ± 15 [a]
3	n.d. [b]
8	n.d. [b]
9	n.d. [b]
11	145 ± 23
14	2.6 ± 0.2

[a] determined with gplTG2

[b] n.d. : inhibition not detected at the compound's solubility limit

View Article Online
DOI: 10.1039/C6MD00565A

Replacement of the enone moiety of ***m*-CP30a**

The α,β-unsaturated carbonyl motif was also mimicked by direct incorporation of an epoxide group or a cyclopropyl group in azachalcone ***m*-CP30a**. A Corey-Chaykovsky cyclopropanation[25] yielded a racemic mixture of the *anti* cyclopropane[26] **15**, as determined by NOESY. A Corey-Chaykovsky epoxidation was used[27] to form epoxide **16**, by replacing the trimethyloxosulfonium iodide used for cyclopropanation with trimethylsulfonium iodide (Scheme 4).

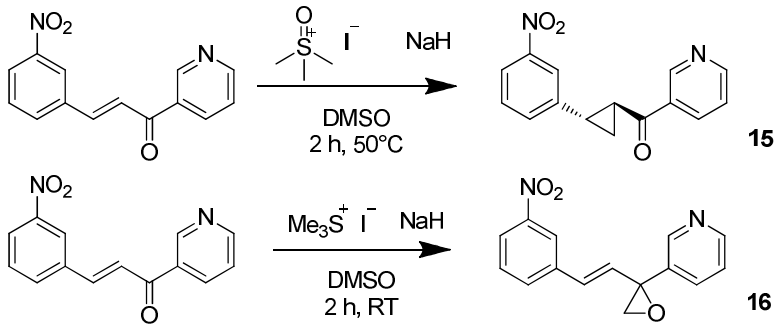

Scheme 4. Synthesis of α,β-unsaturated carbonyl mimics **15** and **16**

Furthermore, an isoxazole mimic was prepared (**17**, Scheme 5), where the heterocycle was formed regioselectively from the α,β-unsaturated ketone *m*-**CP30a** using *N*-hydroxy-4-toluenesulfonamide, according to a published method[28]. The inhibition results for each of these derivatives of *m*-**CP30a** are shown in Table 2.

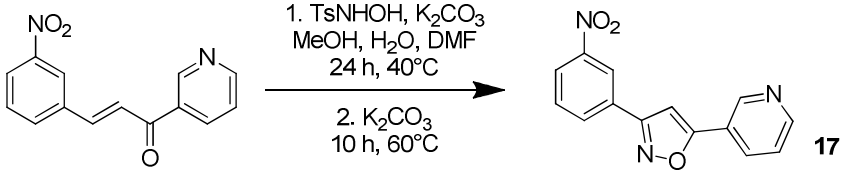

Scheme 5. Synthesis of isoxazole derivative **17**

View Article Online
DOI: 10.1039/C6MD00565A

Table 2. IC_{50} values for the analogues of azachalcone ***m*-CP30a**

Compound	IC_{50} (μM)
***m*-CP30a**	19.6 ± 2.5
15	147 ± 10
16	151 ± 21
17	n.d. [a]

[a] n.d. : inhibition not detected at the compound's solubility limit

Alkyne analogues of **CP4d**

Two alkynyl mimics of **CP4d**, namely **22a** and **22b** (Scheme 6), were also prepared, by replacing the cinnamoyl double bond with a triple bond. Sonogashira coupling between 1-iodo-4-nitrobenzene and propargyl alcohol gave alcohol **18**, which was oxidized with TEMPO to **19**; this aldehyde was then used in a Grignard addition with ethynylmagnesium bromide to form alcohol **20**. A second oxidation with TEMPO afforded[29] ketone **21**, which was then used in a copper(I)-catalysed azide-alkyne cycloaddition (CuAAC), with either benzyl azide (leading to **22a**) or 4-nitrobenzyl azide (leading to **22b**). These azides were previously prepared[16] from the reaction of the corresponding benzyl bromide with sodium azide in DMSO and used without further purification. The inhibition results for these alkynyl derivatives are shown in Table 3. Notably, like its parent inhibitor **CP4d**, compound **22b** was determined via our NMR assay to be equally, if not more, susceptible to GSH addition (see Figure S3 in SI).

View Article Online
DOI: 10.1039/C6MD00565A

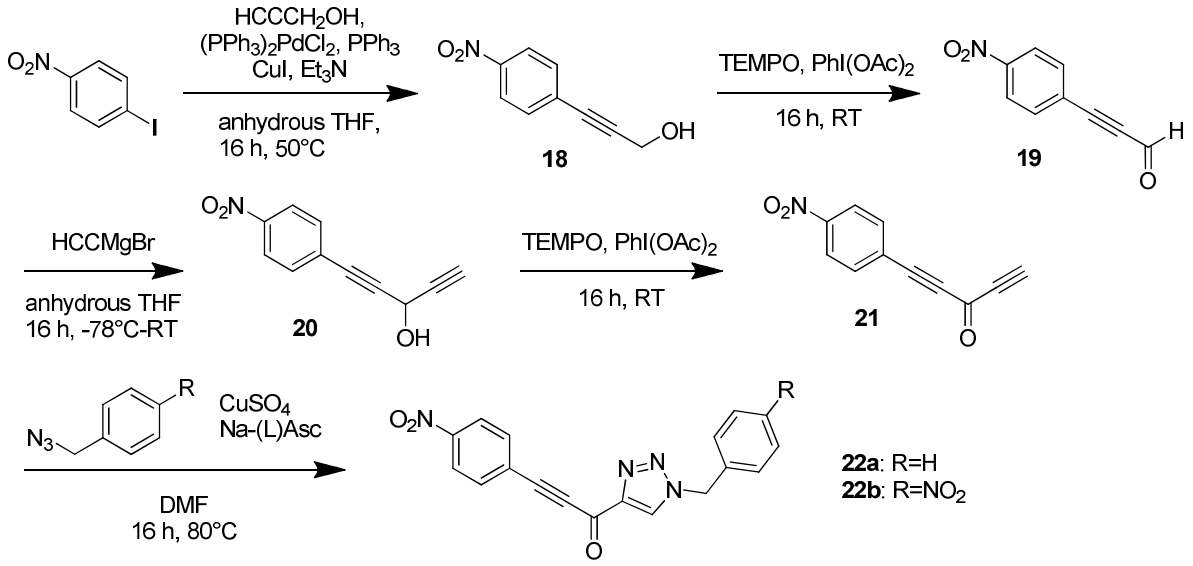

Scheme 6. Synthesis of alkyne analogues **22a** and **22b**

Table 3. IC_{50} results for the alkyne analogues of **CP4d**

Compound	IC_{50} (μM)
CP4d	2.1 ± 0.3[a]
22a	0.61 ± 0.05
22b	0.79 ± 0.05

[a] determined with gplTG2

Bis(triazole) derivatives of **CP4d**

In a final series of analogues, the electrophilic π bonds of inhibitors **CP4d**, **22a**, and **22b**, were replaced with a second triazole ring (Scheme 7, Table 4). A library of derivatives was constructed by maintaining one 4-nitrobenzyl group and varying the ring substituent of the opposite triazole. We began with a CuAAC between 4-nitrobenzylazide and propargyl alcohol, to form alcohol **23**, and then used the same three steps as in the synthesis of **22**, namely the first oxidation with TEMPO to form aldehyde **24**, Grignard addition with ethynylmagnesium bromide

View Article Online
DOI: 10.1039/C6MD00565A

to prepare alcohol **25**, and a second oxidation with TEMPO to form ketone **26**. For both oxidation steps, trichloroisocyanuric acid (TCICA) was used[30] as a radical-regenerating reactant instead of the previously-used (diacetoxyiodo)benzene, due to the low yields obtained with the latter. Another CuAAC was used to form the second triazole, with various substituents, mostly *para* substituted aromatics (Table 4). Given the low IC_{50} obtained with compound **27e**, we also prepared symmetrical compound **27m**, using a similar approach as for the rest of the library. Again, the substituted azides were prepared[16] as described previously. The inhibition data for this bis(triazole) library of compounds are shown in Table 4. Compound **27d** was also analysed for resistance to GSH addition; gratifyingly, we observed no reaction by NMR over 72 hours (see Figure S4 in SI).

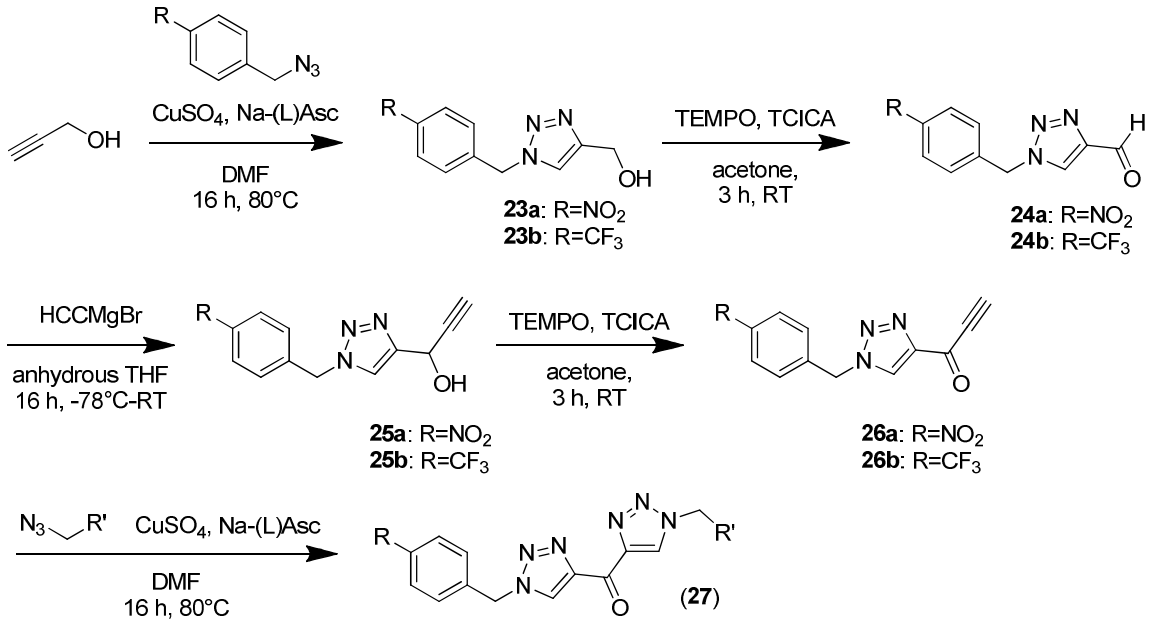

Scheme 7. Synthesis of the library of bis(triazole) compounds

View Article Online
DOI: 10.1039/C6MD00565A

Table 4. IC_{50} values for bis(triazole) compounds

Compound	R group	R' group	IC_{50} (μM)
CP4d	N/A	N/A	2.1 ± 0.3
27a	$-NO_2$	-Ph	n.d. [a]
27b	$-NO_2$	$-(2-NO_2)Ph$	64.1 ± 4.6
27c	$-NO_2$	$-(3-NO_2)Ph$	> 100 [b]
27d	$-NO_2$	$-(4-NO_2)Ph$	14.1 ± 1.7
27e	$-NO_2$	$-(4-CF_3)Ph$	25.9 ± 1.8
27f	$-NO_2$	$-(4-OCF_3)Ph$	> 100 [b]
27g	$-NO_2$	-(4-CN)Ph	> 100 [b]
27h	$-NO_2$	$-(4-CH_3)Ph$	n.d. [a]
27i	$-NO_2$	$-(4-OCH_3)Ph$	n.d. [a]
27j	$-NO_2$	-(4-F)Ph	n.d. [a]
27k	$-NO_2$	-(4-Br)Ph	n.d. [a]
27l	$-NO_2$	-cyclohexyl	n.d. [a]
27m	$-CF_3$	$-(4-CF_3)Ph$	n.d. [a]

[a] n.d. : inhibition not detected at the compound's solubility limit

[b] >100 denotes weak but detectable inhibition at the compound's solubility limit

View Article Online
DOI: 10.1039/C6MD00565A

Discussion

In our first series of mimics, the C=C double bond of the cinnamoyl moiety of **CP15a** was modified by β-alkylation (Figure 2). We hypothesized that the added alkyl group at the β-position would reduce reactivity through steric hindrance and through its electron-donating effect. However, evaluation of these alkylated inhibitors against hTG2 (as described in the Experimental Section) showed that alkylation led to a complete loss of potency (Table 1). To verify that the absence of inhibition was not due to a combination of one isomer being much more potent than the other, we tested compounds **8** (isopropyl, *E*-isomer) and **9** (isopropyl, *Z*-isomer) separately, but noted no detectable inhibition for either one. Given their lack of inhibitory potency, we did not evaluate these compounds for resistance against glutathione.

In a different approach to reduce electrophilicity of the α,β-unsaturated carbonyl motif, we introduced two three-membered rings: a cyclopropane (**15**) to mimic the C=C double bond, and an epoxide (**16**) to mimic the carbonyl. With analogue **15**, a *trans* cyclopropyl group was used to replace the *trans* double bond, while retaining the carbonyl. This modified compound showed a significant loss of potency in comparison to parent ***m*-CP30a**, as did analogue **16**. The latter loss in inhibitory efficiency may be due to the significant change in geometry around the oxygen. Furthermore, despite the replacement of the carbonyl with an epoxide, **16** is arguably equally as susceptible to nucleophilic attack as ***m*-CP30a;** addition to **16** could occur either by direct nucleophilic attack on the epoxide, or by an S_N2' mechanism, where nucleophilic attack on the β carbon of the alkene moiety occurs prior to the opening of the epoxide. Considering how weakly these analogues inhibit hTG2 (Table 2), we did not evaluate them for glutathione resistance.

View Article Online
DOI: 10.1039/C6MD00565A

In our next attempt to design potent inhibitors with diminished susceptibility to glutathione addition, the α,β-double bond of the parent inhibitor was incorporated into a heteroaromatic ring. A coumarin group was used as a mimic of the cinnamoyl group in **CP15a**, yielding compound **11**. Given its 10-fold loss of potency compared to the parent compound, we did not test it for glutathione resistance. We also incorporated an isoxazole ring (**17**) in parent ***m*-CP30a**, where the heterocycle has increased stability as conferred by aromaticity. Furthermore, unlike analogue **16**, derivative **17** maintains the sp^2 hybridisation state of the carbonyl-mimicking oxygen, which helps maintain a similar compound geometry.

However, this compound showed no inhibition of hTG2, possibly due to the geometric constraints associated with the introduction of the isoxazole. Again, given the loss in inhibitory potency (Table 1 and Table 2), we did not evaluate these compounds for resistance to glutathione.

In an effort to remain closer in structure to parent compound **CP15a**, we replaced its double bond with a triple bond, leading to compound **14**. We hypothesized that the greater electronic density surrounding the *sp*-hybridised carbons may decrease their electrophilic reactivity with glutathione. This modified inhibitor was the first to display increased potency (Table 1) when compared to its parent **CP15a**. Encouraged by these initial results, we also prepared an alkyne analogue of **CP4d**, **22b**, and an analogue without the nitro group on the triazole-side benzyl group, **22a**. Similar substitutions were done in the original study[16] and, since nitro groups are generally disfavoured[31] in drug development due to the significant secondary effects related to their metabolism, we wanted to evaluate the importance of the second nitro group on this scaffold. Just like ynone **14**, both these compounds showed high potency against hTG2 (Table 3). We also confirmed that, like its parent **CP4d**, **22b** is also a

View Article Online
DOI: 10.1039/C6MD00565A

competitive inhibitor (Table 5). While these alkynyl compounds were observed by ^{1}H NMR to be as susceptible to GSH addition as the parent **CP4d**, they remain the most potent inhibitors we have prepared to date.

Finally, starting from **CP4d** and **22b**, we replaced the electrophilic double bond with a second triazole group, resulting in the bis(triazole) **27d**. We reasoned that the aromaticity of the heterocycle would diminish the double bond's electrophilicity and confer resistance against GSH addition. In accordance with that hypothesis, we noted no adduct formation over 72 hours in our GSH ^{1}H NMR assay (Figure S4 in SI). Following this positive result, we prepared a library of analogues. Considering that **CP15a** and **CP4d** have a *para*-nitro substitution, but that compound ***m*-CP30a** has a *meta*-nitro group, we first determined the optimal position for substitution on this scaffold. While all three of **27b**, **27c**, and **27d** showed inhibition towards hTG2, unlike the mono-nitro parent **27a**, the results show that, for this scaffold as well, substitution at the *para* position is optimal for inhibitory potency. Based on the encouraging results with **27e**, we also prepared the symmetrical compound **27m**. However, the replacement of the second nitro group with a trifluoromethyl group resulted in complete loss of inhibition.

In comparing each of the most potent scaffolds (alkene, alkyne and triazole), we confirmed that the competitive inhibition observed with parent **CP4d** was maintained with each of the dinitro analogues **22b** and **27d**,. Apparent Michaelis-Menten constants (K_M^{app}) were determined by varying substrate (**AL5**) concentrations for a series of inhibitor concentrations (Figure 2A for **22b**, Figure S5 in SI for **27d**). Plotting both K_M^{app} and V_{max} against inhibitor concentration (Figure 2B, Figure S6 in SI for **27d**) confirmed the competitive mode of inhibition, and allowed us to determine K_i. A similar approach was used with **27d**, leading to the data shown in Table 5.

View Article Online
DOI: 10.1039/C6MD00565A

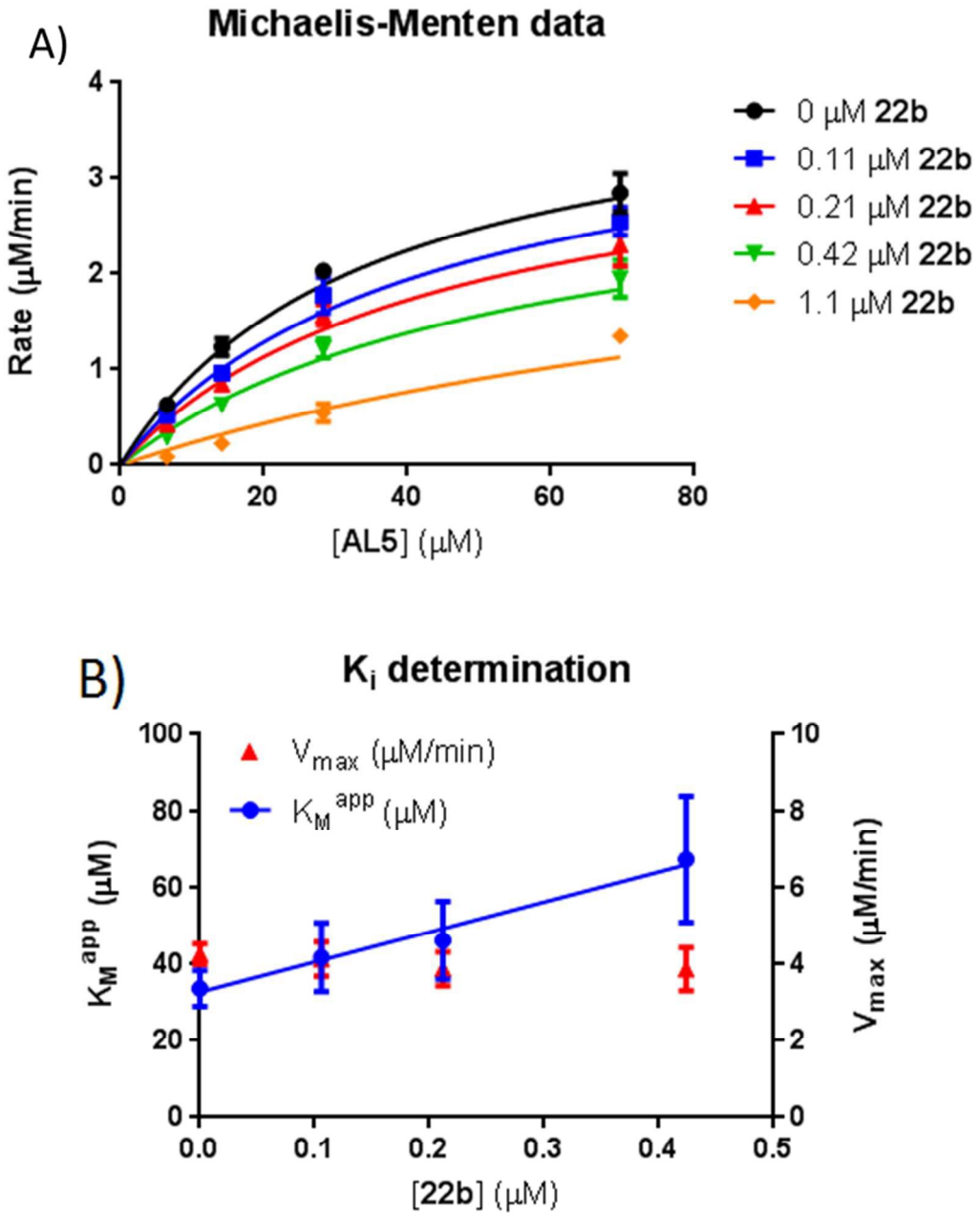

Figure 3. Determination of the inhibition constant for **22b** a) Michaelis-Menten curves at various concentrations of inhibitor and b) Determination of the mode of inhibition and value of K_i

View Article Online
DOI: 10.1039/C6MD00565A

Table 5. Inhibition constants (K_i) for selected inhibitors towards human TG2

Compound	K_i (μM)
CP4d	1.0 ± 0.1[17]
22b	0.42 ± 0.05
27d	9.9 ± 1.6

While **27d** showed a reduction in affinity of one order of magnitude compared to parent **CP4d**, this decrease is accompanied by an increased resistance to GSH addition, which is a significant concern in the targeting of intracellular hTG2. In comparison, inhibitor **22b** is our most potent reversible hTG2 inhibitor to date, with the first sub-micromolar K_i value, at 420 nM. This compound would be particularly appropriate for the inhibition of extracellular hTG2, where the concentration of GSH is much lower and less likely to react with our compound.

Conclusion

In summary, we have developed a rapid ^{1}H-NMR-based assay to measure the reactivity of our reversible hTG2 inhibitors with GSH. Given the significant extent of reactivity observed with the parent inhibitors, their scaffolds were modified to reduce their electrophilicity. In this study, two notable new scaffolds were developed: alkynes and bis(triazoles). The former compounds, including **22b** with a K_i of 420 nM, show great promise as competitive inhibitors of extracellular hTG2, given that the extracellular concentration of GSH is one to three orders of magnitude lower than inside cells, reaching values below 5 μM in plasma[32]. The latter scaffolds show potential for targeting intracellular hTG2 by virtue of their increased resistance to GSH addition. Future work will involve development of these scaffolds and *in cellulo* evaluation.

View Article Online
DOI: 10.1039/C6MD00565A

Acknowledgements

This work was supported financially by the Natural Sciences and Engineering Research Council of Canada (NSERC). K.Y.P.A. is grateful to the University of Ottawa for an Admission (Excellence) scholarship and to the Fonds de Recherche Québécois: Nature et Technologies (FRQNT) for a doctoral scholarship. I.R. is grateful to NSERC and the Fonds Québecois de Recherche sur la Nature et les Technologies (FQRNT) for postgraduate scholarships. V.S., N.B.-F., S.-P.P. and E.D.F. are grateful to NSERC for Undergraduate Summer Research Awards (USRA).

Supporting Information

Synthetic methods, spectra for the NMR assay and graphs for the determination of the K_i value for **27d** are included.

Kinetic methods

Evaluation of resistance to glutathione by ^{1}H NMR

^{1}H NMR spectra of a solution of 12 mM inhibitor and 80 mM glutathione in DMSO-d_6 (1 mL) were recorded on a Bruker AVANCE 300 spectrometer at the indicated time points. Spectra were collected for each substrate individually, as well as after combining the inhibitor and GSH, at 10 minutes, one hour, two hours and four hours to monitor any changes different from an additive spectrum. The product was then analysed by mass spectrometry to confirm the presence the proposed glutathione adduct.

HRMS (ESI$^+$) for **1**: $[C_{24}H_{27}N_5O_9S+Na]^+$ calc. 584.1422 Da, obt. 584.1500 Da

View Article Online
DOI: 10.1039/C6MD00565A

Determination of IC_{50} values

Kinetic runs were recorded on a Varian Cary 100 Bio UV-visible spectrophotometer at 405 nm and 25°C, in a buffer composed of 111 mM MOPS (pH 7.0), 3.33 mM $CaCl_2$, and 0.05 mM EDTA. All aqueous solutions were prepared using deionised water. Each kinetic assay was performed using 900 µL buffer, 25 µL of a DMF stock solution of substrate *N*-Cbz-Glu(γ-*p*-nitrophenylester)Gly (**AL5**)[33] (1 mg/mL, 2.2 mM), 50 µL of a solution of hTG2 at 0.05 U/mL (final concentration of 2.5 mU/mL) and 0-25 µL of a DMF stock solution of inhibitor (contingent on solubility; the highest concentration tested was generally between 5 and 30 µM). The volume of DMF was then adjusted so that it represented 5% of the final volume. The reaction was initiated with the addition of hTG2 (expressed and purified according to a literature protocol[17]), and the increase in absorbance was monitored over 10 minutes; initial rates were measured over the first five minutes of absorbance change. IC_{50} values were obtained as the negative x-intercept of a Dixon plot (reciprocal of initial rates vs. inhibitor concentration).

Determination of K_i values

Kinetic runs were recorded on a UV-visible spectrophotometer at 405 nm and 25°C, in a buffer composed of 111 mM MOPS (pH 7.0), 3.33 mM $CaCl_2$, and 0.05 mM EDTA. All aqueous solutions were prepared using deionised water. Stock solutions of **AL5** (1 mg/mL, 2.2 mM) and inhibitor (0.65 mg/mL, 1.50 mM for compound **27d** and 0.04 mg/mL, 0.11 mM for **22b**) were prepared in DMF. For each solution, the volume of DMF was adjusted to represent 5% of the final volume, and 2.5 mU/mL of hTG2 were used to run the assay. Michaelis-Menten curves were determined using **AL5** concentrations of 6.5 µM, 14 µM, 28 µM and 70 µM (representing 0.5, 1, 2 and 5 times K_M (14 µM[18])), and inhibitor concentrations of 1.5 µM, 3.0 µM, 6.0 µM and 15 µM for compound **27d** or 0.11 µM, 0.21 µM, 0.42 µM and 1.1 µM for **22b**. The reaction was

View Article Online
DOI: 10.1039/C6MD00565A

initiated with the addition of hTG2 (expressed and purified according to a literature protocol[17]), and the increase in absorbance was monitored over 10 minutes; initial rates were measured over the first five minutes of absorbance change. Michaelis-Menten curves were fitted by non-linear regression to equation 1, using Graph Pad Prism 6, to obtain K_M^{app} values, while K_i values were then determined by linear regression of K_M^{app} vs. inhibitor concentration, using equation 2.

$$v = \frac{V_{max}[AL5]}{K_M^{app}+[AL5]} \quad \text{Eq. 1}$$

$$K_M^{app} = K_M\left(1+\frac{[inhibitor]}{K_i}\right) = \frac{K_M}{K_i}[inhibitor] + K_M \quad \text{Eq. 2}$$

View Article Online
DOI: 10.1039/C6MD00565A

References

1. C. M. Clouthier, G. G. Mironov, V. Okhonin, M. V. Berezovski and J. W. Keillor, *Angew. Chem., Int. Ed.*, 2012, **51**, 12464-12468.
2. D. M. Pinkas, P. Strop, A. T. Brunger and C. Khosla, *PLoS Biol.*, 2007, **5**, 2788-2796.
3. L. Fesus and M. Piacentini, *Trends Biochem. Sci.*, 2002, **27**, 534-539.
4. X. Jin, J. Stamnaes, C. Kloeck, T. R. Di Raimondo, L. M. Sollid and C. Khosla, *J. Biol. Chem.*, 2011, **286**, 37866-37873.
5. J. W. Keillor, C. M. Clouthier, K. Y. P. Apperley, A. Akbar and A. Mulani, *Bioorg. Chem.*, 2014, **57**, 186-197.
6. M. Griffin, R. Casadio and C. M. Bergamini, *Biochem. J.*, 2002, **368**, 377-396.
7. J. Tucholski, M. Lesort and G. V. W. Johnson, *Neuroscience (Oxford, United Kingdom)*, 2001, **102**, 481-491.
8. Z. Balajthy, K. Csomos, G. Vamosi, A. Szanto, M. Lanotte and L. Fesus, *Blood*, 2006, **108**, 2045-2054.
9. Z. Sarang, P. Molnar, T. Nemeth, S. Gomba, T. Kardon, G. Melino, S. Cotecchia, L. Fesus and Z. Szondy, *Hepatology (Hoboken, NJ, U. S.)*, 2005, **42**, 578-587.
10. L. K. Boroughs, M. A. Antonyak and R. A. Cerione, *J. Biol. Chem.*, 2014, **289**, 10115-10125.
11. G. Melino, M. Annicchiarico-Petruzzelli, L. Piredda, E. Candi, V. Gentile, P. J. A. Davies and M. Piacentini, *Mol. Cell. Biol.*, 1994, **14**, 6584-6596.
12. C. A. Gaudry, E. Verderio, D. Aeschlimann, A. Cox, C. Smith and M. Griffin, *J. Biol. Chem.*, 1999, **274**, 30707-30714.
13. L. Lorand and R. M. Graham, *Nat. Rev. Mol. Cell Biol.*, 2003, **4**, 140-156.
14. C. Pardin, S. M. F. G. Gillet and J. W. Keillor, *Bioorg. Med. Chem.*, 2006, **14**, 8379-8385.
15. C. Pardin, J. N. Pelletier, W. D. Lubell and J. W. Keillor, *J. Org. Chem.*, 2008, **73**, 5766-5775.
16. C. Pardin, I. Roy, W. D. Lubell and J. W. Keillor, *Chem. Biol. Drug Des.*, 2008, **72**, 189-196.
17. I. Roy, O. Smith, C. M. Clouthier and J. W. Keillor, *Protein Expres. Purif.*, 2013, **87**, 41-46.

View Article Online
DOI: 10.1039/C6MD00565A

18. I. Roy, Ph.D., Université de Montréal, 2014.
19. B. Budke, J. H. Kalin, M. Pawlowski, A. S. Zelivianskaia, M. Wu, A. P. Kozikowski and P. P. Connell, *J. Med. Chem.*, 2013, **56**, 254-263.
20. E. Carceller, J. Salas, M. Merlos, M. Giral, R. Ferrando, I. Escamilla, J. Ramis, J. Garcia-Rafanell and J. Forn, *J. Med. Chem.*, 2001, **44**, 3001-3013.
21. A. Song, X. Wang and K. S. Lam, *Tetrahedron Lett.*, 2003, **44**, 1755-1758.
22. K. Sonogashira, Y. Tohda and N. Hagihara, *Tetrahedron Lett.*, 1975, 4467-4470.
23. T. Eckert and J. Ipaktschi, *Synth. Commun.*, 1998, **28**, 327-335.
24. A. R. Katritzky, Y. Zhang and S. K. Singh, *Synthesis*, 2003, 2795-2798.
25. E. J. Corey and M. Chaykovsky, *J. Am. Chem. Soc.*, 1965, **87**, 1353-1364.
26. R. J. Paxton and R. J. K. Taylor, *Synlett*, 2007, 633-637.
27. E. J. Corey and M. Chaykovsky, *J. Am. Chem. Soc.*, 1962, **84**, 3782-3783.
28. S. Tang, J. He, Y. Sun, L. He and X. She, *Org. Lett.*, 2009, **11**, 3982-3985.
29. D. J. Vugts, L. Veum, K. al-Mafraji, R. Lemmens, R. F. Schmitz, F. J. J. de Kanter, M. B. Groen, U. Hanefeld and R. V. A. Orru, *Eur. J. Org. Chem.*, 2006, 1672-1677.
30. S. I. Presolski, V. Hong, S.-H. Cho and M. G. Finn, *J. Am. Chem. Soc.*, 2010, **132**, 14570-14576.
31. C.-H. Hsu, T. Stedeford, E. Okochi-Takada, T. Ushijima, H. Noguchi, C. Muro-Cacho, J. W. Holder and M. Banasik, *J. Environ. Sci. Health, Part C Environ. Carcinog. Ecotoxicol. Rev.*, 2007, **25**, 155-184.
32. B. Halliwell and J. M. C. Gutteridge, *Free Radicals in Biology and Medicine*, Oxford University Press, 2015.
33. A. Leblanc, C. Gravel, J. Labelle and J. W. Keillor, *Biochemistry*, 2001, **40**, 8335-8342.

View Article Online
DOI: 10.1039/C6MD00565A

Graphical Table of Contents entry

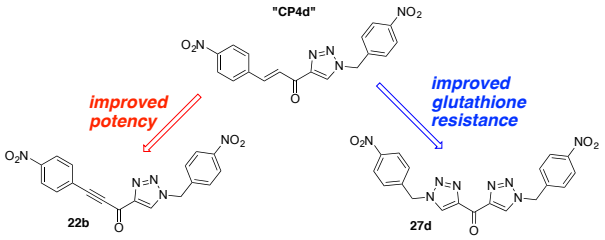

Starting from known reversible inhibitor **CP4d**, we have designed two new classes of inhibitors, improving both potency (**22b**) and glutathione resistance (**27d**).